6. A. Dalgleish *et al.*, *Nature (London)* **312**, 763; D. Klatzmann *et al.*, *ibid.*, p. 767; J. McDougal *et al.*, *J. Immunol.* **135**, 3151 (1985).
7. J. McDougal *et al.*, *Science* **231**, 382 (1986).
8. P. Maddon *et al.*, *Cell* **47**, 333 (1986).
9. J. Lifson, G. Reyes, M. McGrath, B. Stein, E. Engleman, *Science* **232**, 1123 (1986).
10. B. Yoffe *et al.*, *Proc. Natl. Acad. Sci. U.S.A.* **84**, 1429 (1987).
11. J. Sodroski, W. Goh, C. Rosen, K. Campbell, W. Haseltine, *Nature (London)* **322**, 470 (1986); J. Lifson *et al.*, *ibid.* **323**, 725 (1986).
12. J. Coffin, *Cell* **46**, 1 (1986).
13. H. Mitsuya and S. Broder, *Nature (London)* **325**, 773 (1987).
14. L. Goodman and A. Gilman, *The Pharmacologic Basis of Therapeutics* (Macmillan, New York, ed. 5, 1975).
15. L. Lasky *et al.*, *Cell* **50**, 975 (1987).
16. L. Lasky *et al.*, *Science* **233**, 209 (1986).
17. R. Gallo *et al.*, *ibid.* **224**, 500 (1984).
18. H. Lyerly *et al.*, *Proc. Natl. Acad. Sci. U.S.A.* **84**, 4601 (1987).
19. Cells were transfected with plasmids encoding CD4, CD4T, or GDCD4T by a modification of the calcium phosphate procedure (*20*). Confluent 60-mm plates were labeled 48 hours later with 1.2 ml of methionine-free DME medium containing 1 mCi of [^{35}S]methionine (1200 Ci/mmol) for 6 hours. Culture supernatants were collected, clarified by low speed centrifugation, and diluted with an equal volume of 2× RIPA buffer, cells were washed with phosphate-buffered saline and then dissolved in 1 ml of 1× RIPA buffer (1% Triton X-100, 0.5% sodium deoxycholate, 0.1% SDS, 0.12*M* NaCl, 0.05*M* tris-HCl, *p*H 7.5). Samples were preadsorbed with 5 μl of normal rabbit serum for 1 hour at 4°C and cleared with 40 μl of Pansorbin (10% w/v, Calbiochem) for 30 minutes at 4°C. Samples were then incubated overnight at 4°C with 2 μl of normal serum or 5 μl (0.25 μg) of OKT4 (Ortho Diagnostics), and immune complexes were then collected with 10 μl of Pansorbin. Precipitates were washed twice in 1× RIPA and once in water, then eluted by heating at 100°C for 2 minutes in sample buffer (0.12*M* tris-HCl, *p*H 6.8, 0.7*M* β-mercaptoethanol, 20% glycerol, 4% SDS, and 0.1% bromophenol blue). Immunoprecipitated proteins were resolved on SDS-polyacrylamide gels and visualized by fluorography (*20*).
20. M. Muesing *et al.*, *Cell* **48**, 691 (1987).
21. Coimmunoprecipitation of CD4-gp120 complexes was performed by a modification of the procedure of McDougal *et al.* (*7*). Binding reactions consisted of ^{35}S-labeled rgp120 incubated at 4°C for 1 hour with either lysates of cells expressing intact CD4 or supernatants from cells containing CD4T or GDCD4T or from mock-transfected cells. Alternatively, supernatants containing ^{35}S-labeled CD4T or GDCD4T were incubated with supernatants from cells containing unlabeled rgp120 (*16*) or untransfected cells. Binding reactions had a final composition of 0.5× McDLB (1× McDLB is 0.5% NP40, 0.2% sodium deoxycholate, 0.12*M* NaCl, 0.02*M* tris-HCl, *p*H 8.0). Reactions were immunoprecipitated and analyzed as described above (*24*) except that washes were carried out with 1× McDLB.
22. Purified soluble rgp120 (*16*) was radioiodinated with lactoperoxidase to a specific activity of 2.9 nCi/ng. Binding reactions consisted of ^{125}I-gp120 (3 ng to 670 ng) incubated for 1 hour at 4°C with cell lysates containing intact CD4 or cell supernatants containing unlabeled CD4T or GDCD4T (*19*). Reactions (0.2 ml) had a final composition of 0.5× McDLB, and were performed in duplicate, both in the presence or absence of 50 μg of unlabeled purified rgp120 (*16*). After incubation, bound gp120 was quantitated by immunoprecipitation (*19*), and counted in a gamma counter. Data were analyzed by the Scatplot program written by R. Vandlen, Genentech, Inc.
23. M. Robert-Guroff, M. Brown, R. Gallo, *Nature (London)* **316**, 72 (1985).

24. We thank E. Peralta, J. Winslow, and P. Moore for discussions; C. Lucas and S. Frei for providing ^{125}I-gp120; M. Vasser, P. Jurhani, and P. Ng for oligodeoxynucleotide synthesis; and C. Morita and W. Anstine for preparation of the figures.

6 October 1987; accepted 30 October 1987

Three-Dimensional Structure of Interleukin-2

BARBARA J. BRANDHUBER, TOM BOONE, WILLIAM C. KENNEY, DAVID B. MCKAY*

Interleukin-2 is an effector protein that participates in modulating the immune response; it has become a focal point for the study of lymphokine structure and function. The three-dimensional structure of the interleukin molecule has been solved to 3.0 angstrom resolution. Interleukin-2 has a novel alpha-helical tertiary structure that suggests one portion of the molecule forms a structural scaffold, which underlies the receptor binding facets of the molecule.

INTERLEUKIN-2 (IL-2) IS A LYMPHOkine protein produced by antigen- or mitogen-stimulated T lymphocytes whose first documented activity is to stimulate proliferation of IL-2–dependent T cells (*1*). It modulates immunological effects on cytotoxic T cells (*2, 3*), natural killer cells (*4, 5*), activated B cells (*6, 7*) and lymphokine-activated cells (*8, 9*). IL-2 asserts its effect by binding a specific high affinity receptor on the surface of target cells; consequently, the IL-2 molecule has become a focal point for studying receptor-effector interactions that modulate cell proliferation in the immune response.

The high affinity ($K_D \sim 10^{-11} M$) receptor responsible for mediating the effect of IL-2 on target cells consists of two distinct membrane-bound proteins of size 55 kD (p55 or Tac) and 75 kD (p75); each of these two proteins can act by itself as an apparent low affinity ($K_D \sim 10^{-8} M$) receptor for IL-2, and both are required for IL-2 activity (*10*). This suggests that IL-2 must simultaneously bind both p55 and p75 to form a trimeric complex for activity, and by inference, that IL-2 must have two separate receptor binding sites.

Knowledge of the three-dimensional structure of IL-2 should provide a foundation for systematic delineation of its receptor binding sites, as well as an evaluation of the accuracy of recent predictions of its structure (*11, 12*). We reported earlier the low (5.5 Å) resolution structure of IL-2 (*13*); we have extended these crystallographic results to 3.0 Å resolution, and now describe the overall tertiary structure of IL-2.

The purification, crystallization, and initial structure determination to 5.5 Å resolution of human recombinant IL-2, as well as structural work reported by others, have been described (*13*). Briefly, we have found that IL-2 and an analog in which Cys^{125} has been replaced with alanine ([Ala^{125}]IL-2) crystallize isomorphously in the triclinic space group *P1*, with unit cell parameters **a** = 55.8 Å, **b** = 40.1 Å, **c** = 33.7 Å, α = 90.0°, β = 109.3°, and γ = 93.2°. The unit cell contains two molecules related by near-2_1 symmetry. With rare exception, an unusual twinning of the crystals leads to overlap of reflections from the two contributing twins for reciprocal lattice indices $k = 0, \pm 6, \pm 7, \pm 12, \pm 13, \ldots$.

Data were collected by diffractometer, processed, and scaled (*13*); multiple heavy atom isomorphous replacement (MIR) phasing statistics are summarized in Table 1. Two crystals that were essentially single (showed no significant twinning) allowed us to collect data on reflections that overlap in twinned crystals for the native and mercury phenyl glyoxal data sets in [Ala^{125}]IL-2 crystals to 3.5 Å resolution. Reflections that overlapped because of the crystal twinning for the other heavy atom derivatives were discarded from the computations.

Solvent flattening was used to improve the quality of the 3.0 Å phases. In our implementation of the method, envelopes outlining each molecule in the unit cell were constructed and digitized; the envelope encompassed 27.3 percent and 27.0 percent of the cell volume for the first and second molecule, respectively, leaving 45.7 percent as solvent. Iteratively, maps were computed on a 1 Å grid, the solvent density was set equal to its average value, and the protein density was left unmodified; the solvent-flattened map was Fourier-transformed to produce calculated structure factors (F_{calc}), the $|F_{calc}|$'s were scaled in shells of resolution to the measured native structure factor magnitudes ($|F_{obs}|$), and Sim-weighted calculated phases were combined with MIR phases by direct multiplication of their phase probability distributions to yield combined phases. The combined phases were then used to calculate a new map.

After several cycles, the overall agreement between observed and calculated structure factors,

$$R = \Sigma||F_{calc}| - |F_{obs}||/\Sigma|F_{obs}|$$

summed over all contributing reflections,

B. J. Brandhuber and D. B. McKay, Department of Chemistry and Biochemistry, University of Colorado, Boulder, CO 80309.
T. Boone and W. C. Kenny, Amgen, 1900 Oak Terrace Lane, Thousand Oaks, CA 91320.

*To whom correspondence should be sent.

converged from an initial value of 0.374 to a final value of 0.209. The final R factor was essentially level over the resolution range 30.0 Å to 3.0 Å. The overall root-mean-square (rms) change in phase angle for combined phases between the final and penultimate cycles was 10.9°; the final rms phase difference between combined and MIR phases rose gradually with increasing resolution from 25° in the 30 Å to 10 Å resolution range to 66° in the 3.1 Å to 3.0 Å range.

Models for both of the molecules in the unit cell have been constructed independently with an Evans and Sutherland PS-300 graphics system with the aid of the model building program FRODO. Throughout the model building, the two molecules were cross-checked for consistency. Most of the polypeptide backbone could be readily traced in the solvent flattened map. Placing the sequence was aided by four "tether points". We identified Cys^{125} as a specific site of reaction on each molecule found with several heavy atom reagents (terpyridine platinum, mercury phenyl glyoxal, and 1-fluoro-2,4-dibromobenzene) in crystals of IL-2 but not in crystals of [Ala^{125}]IL-2. The disulfide, apparent for both molecules in the 3.0 Å map, located Cys^{58} and Cys^{105}. The major site of iodination of IL-2 in solution has been reported to be Tyr^{45} (*14*); we have found the two major sites of iodination in our crystals to be contiguous with the side chain density of residues traced as Tyr^{45} in the two molecules; further, the "bend" in the helix containing Tyr^{45} correlates with the direction of helix bend expected from the placement of Pro^{47} (described below).

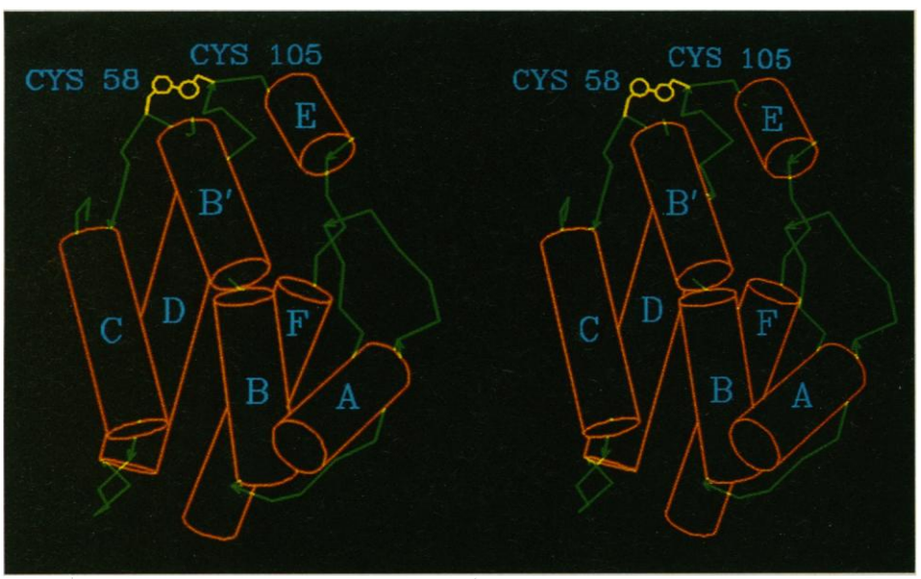

Fig. 1. Schematic stereo drawing of IL-2; helices are represented as cylinders and are lettered sequentially from the amino terminus. Picture produced by a program written by A. M. Lesk and K. D. Hardman (*24*).

Table 1. Data collection and heavy atom refinement statistics on native and derivative crystals.

Crystal	Derivative	Maximum resolution (Å)	R_{sym}	Completeness of data*	f_{rms}/E_{rms}
[Ala^{125}]IL-2	Native	3.0	0.048	0.88	
[Ala^{125}]IL-2	1 m*M* mercury phenyl glyoxal, 1 day	3.5	0.060	0.96	0.96
IL-2	1 m*M* mercury phenyl glyoxal, 1 day	3.2	0.073	0.78	1.24
IL-2	5 m*M* 2,2′,2″-terpyridyl platinum(II), 2½ days	3.0	0.047	0.78	0.96
[Ala^{125}]IL-2	1 m*M* Na_2WO_4, 1 day	3.5	0.036	0.80	0.94
[Ala^{125}]IL-2	Iodination	4.0	0.064	0.77	1.24
				Figure of merit	0.68
				Number of reflections	4759

*Fraction of reflections measured to maximum resolution after overlaps discarded.

$$R_{sym} = \Sigma_{hkl} \Sigma_{obs} (I_{obs} - \langle I \rangle_{hkl}) / \Sigma_{hkl} \Sigma_{obs} \langle I \rangle_{hkl}$$

$$f_{rms} = [\Sigma_{hkl} f_H^2 / n]^{1/2}$$

$$E_{rms} = [\Sigma_{hkl} (F_{PH} - |F_P + f_H|)^2 / n]^{1/2}$$

where I_{obs} = measured diffraction intensity and $\langle I \rangle_{hkl}$ = mean value of all intensity measurements of (h, k, l) reflection; f_H = calculated heavy atom structure factor; F_P = square root of measured native intensity; F_{PH} = square root of measured derivative intensity; n = total number of reflections contributing to sum; $\mathbf{F}_P = F_P \exp(i *$ calculated native phase); $\mathbf{f}_H = f_H \exp(i *$ calculated heavy atom phase)

The amino-terminal region proved difficult to trace in both molecules; we have not yet placed the first ten residues unambiguously. We anticipate that molecular refinement and phase extension, with the use of native data we have collected to 2.5 Å, will eventually resolve this ambiguity. Our current model of IL-2 allows us to describe the overall tertiary structure of the molecule and to suggest which facets of the structure may be involved in receptor binding.

IL-2 is an alpha-helical protein (Fig. 1). It has a short helical segment near the amino terminus (residues 11 to 19; helix A in Fig. 1), followed by an extended loop; residues 33 to 56 form a helix interrupted, or "bent," near the middle by Pro^{47} (hence the two segments are referenced as B and B′); following Cys^{58} of the disulfide are helix C, residues 66 to 78, and D, residues 83 to 101; following Cys^{105} is a short, apparently helical stretch E, residues 107 to 113, which leads into the carboxyl-terminal helix F, residues 117 to 133. There are no segments of β secondary structure in the molecule. The overall helical content of ~65 percent is in good agreement with estimates based on circular dichroism (*11, 15*). The disulfide between Cys^{58} and Cys^{105} links two extended loops that connect the helices across the "top" (in the orientation of Fig. 1) of the molecule.

Helices B, C, D, and F form an apparent antiparallel alpha helical bundle which differs significantly from the classical four-helix bundle represented by cytochrome c′, cytochrome b_{562}, and myohemerythrin (*16*). The packing regions of the helices are shorter, involving only three to four turns of helix, while classical four-helix bundles usually have at least five turns in each helix. Further, the packing angles all fall in the range of 25° to 30° (Table 2), and hence are somewhat larger than the average of approximately 18° found in classical four-helix bundles.

We expect murine IL-2 to have a similar structure beginning with helix A and including the proline-induced bend in helix B+B′. This is significant since recombinant human IL-2 shows activity on both human and murine T cells (*17*), and recombinant murine IL-2 is reported to have a low but measurable specific activity on human T cells (*18*). The murine (*19*) and human (*20*) IL-2 sequences have 64 percent overall homology. The amino acid sequence of the mature murine protein is identical to the human sequence for the first seven residues, and then has one or more insertions, a total of 15 amino acids, relative to human, including a 12-residue poly(Gln) stretch, prior to Leu^{14} of human IL-2; hence the amino-

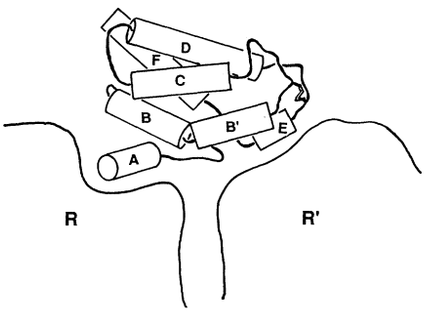

Fig. 2. Schematic drawing showing a possible mode of interaction of IL-2 with two distinct receptors.

terminal region of the murine protein may have significant structural differences from the human protein up to, and possibly including the first turn of, helix A. The only additional insertion in the murine sequence is between human IL-2 residues 80 and 81, in the loop connecting helices C and D.

The current data on IL-2 receptor binding suggest that the molecule "bridges" two receptor molecules, p55 and p75, with two independent binding sites, when bound to its high affinity receptor. Earlier work did not presage the presence of two receptor molecules; hence, modifications that affect IL-2 receptor binding do not discriminate between those involving a p55–(IL-2) interaction, a p75–(IL-2) interaction, or both.

Antibodies to peptides that cross-react with IL-2 have been used to map global regions in the IL-2 sequence likely to be important in receptor binding. In particular, Kuo and Robb have presented evidence suggesting regions within the residue bounds 8 to 27 and 33 to 54 are directly involved in receptor binding (*21*), while Altman and colleagues found that antibodies against peptides of residues 59 to 72, 91 to 105, and 119 to 133 did not inhibit IL-2 receptor binding (*22*). This suggests that a portion of the amino-terminal helix A, helix B+B′, and the peptide connecting them are likely candidates for receptor interaction, while helices C, D, and F are not.

Evidence from amino-terminal deletion modification of IL-2 correlates with this suggestion. In particular, Ju *et al.* have demonstrated that deletion of residues 1 to 10 of human IL-2 (the amino terminus to the beginning of helix A) reduces induction of proliferation of murine CTLL-2 cells by only 30 to 50 percent, whereas deletion of residues 1 to 20 (the amino terminus including helix A) abolishes activity completely (*23*). Deletion analysis of murine IL-2 shows a similar pattern of effects on proliferation activity of murine HT2 T cells (*18*). Deletion of murine residues 1 to 11 or 1 to 13 (prior to helix A, assuming murine IL-2 is structurally similar to human IL-2) reduces activity by at most 50 percent. Deletions of the murine poly(Gln) section, residues 15 to 26, coupled with various changes in sequence in the first 37 amino acids, has resulted in mutant protein with as much as one-third the specific activity of the native protein. However, deletion through murine residue 30 (corresponding to human residue 16, in the middle of helix A) reduces activity to ~0.4 percent that of the native protein, and deletion through residue 41 (corresponding to human residue 27) abolishes activity completely. Hence the amino terminus up to, and possibly including the first few residues of, helix A appears redundant for IL-2 activity; but most, if not all, of the A helix appears essential.

Most of the other reported deletions that abolish activity—many of which would delete a significant fraction of an internal helix in the structure or the peptide connecting them—are such that they probably disrupt the overall tertiary structure of IL-2.

Data on site-specific amino acid substitutions suffer from a lack of distinction between those mutations that affect activity by destabilizing the IL-2 structure and those that directly affect receptor binding. Except for alterations that destroy the disulfide of IL-2 or modify Trp^{121} (whose side chain is internal in the structure), all of the mutations shown to lower activity of human IL-2 are in sequence regions 3 to 17 and 36 to 54 (*23*), which corroborates the receptor binding regions suggested by antibody competition studies. The "down" point mutations, when placed on the IL-2 model, do not identify a specific receptor binding surface.

We would suggest, as a working hypothesis, that helices B, C, D, and F form a structural scaffold, and that helices A, B′ and possibly part of B, and E form the receptor binding sites of IL-2 (Fig. 2). The data discussed above correlate well with the suggested involvement of helices A, B, and B′ in receptor binding. The possible involvement of helix E is suggested primarily because of its spatial accessibility and its proximity to regions of the molecule probably involved in receptor interactions; we have found no data addressing the possible role of residues 106 to 115 in receptor binding. The IL-2 tertiary structure model provides a foundation for systematically testing this suggestion and delineating the receptor binding sites of the IL-2 molecule.

Table 2. Packing angles for helices in IL-2. Alpha carbons of an ideal helix were superimposed on alpha carbons of helices in the IL-2 models; rms discrepancies between ideal and model alpha carbon positions ranged from 0.4 Å to 0.8 Å. Packing angles were computed as the angles between the polar directions of the axes of the helices. Angles were computed for models of both IL-2 molecules in the unit cell, except for A–B, since the A helix is reliably traced in only one molecule; standard deviations of the two measurments are given in parentheses.

A–B	78.6°	
B–C	28.4°	(9.1°)
C–D	28.7°	(1.4°)
D–F	25.6°	(2.1°)
B–F	25.9°	(1.0°)
B′–E	16.2°	(9.8°)

REFERENCES AND NOTES

1. S. Gillis, M. M. Ferm, W. Ou, K. A. Smith, *J. Immunol.* **120**, 2027 (1978).
2. S. Gillis, K. A. Smith, J. Watson, *ibid.* **124**, 1954 (1980).
3. J. M. Zarling and F. H. Bach, *Nature (London)* **280**, 685 (1979).
4. C. S. Henney, K. Kuribayashi, D. E. Kern, S. Gillis, *ibid.* **291**, 335 (1981).
5. J. R. Ortaldo *et al.*, *J. Immunol.* **133**, 779 (1984).
6. M. C. Mingari *et al.*, *Nature (London)* **312**, 641 (1984).
7. B. L. Pike *et al.*, *Proc. Natl. Acad. Sci. U.S.A.* **81**, 7917 (1984).
8. E. A. Grimm, A. Mazumder, H. Z. Zhang, S. A. Rosenberg, *J. Exp. Med.* **155**, 1823 (1982).
9. A. Mazumder and S. A. Rosenberg, *ibid.* **159**, 495 (1984).
10. M. Tsudo, R. W. Kozak, C. D. Goldman, T. A. Waldman, *Proc. Natl. Acad. Sci. U.S.A.* **84**, 4215 (1987).
11. F. E. Cohen *et al.*, *Science* **234**, 349 (1986).
12. V. P. Zav'yalov and A. I. Denesyvk, *Immunol. Lett.* **10**, 71 (1985).
13. B. J. Brandhuber, T. Boone, W. C. Kenney, D. B. McKay, *J. Biol. Chem.* **262**, 12306 (1987).
14. R. J. Robb, P. C. Mayer, R. Garlick, *J. Immunol. Methods* **81**, 15 (1985).
15. T. Arakawa, T. Boone, J. M. Davis, W. C. Kenney, *Biochemistry* **25**, 8274 (1986).
16. J. S. Richardson, *Adv. Protein Chem.* **34**, 167 (1981).
17. S. A. Rosenberg, E. A. Grimm, M. McGrogan, M. Doyle, E. Kawasaki, K. Koths, D. F. Mark, *Science* **223**, 1412 (1984).
18. S. M. Zurawski, T. R. Mosmann, M. Benedik, G. Zurawski, *J. Immunol.* **137**, 3354 (1986).
19. N. Kashima *et al.*, *Nature (London)* **313**, 402 (1985).
20. T. Taniguchi *et al.*, *ibid.* **302**, 305 (1983).
21. L. Kuo and R. J. Robb, *J. Immunol.* **137**, 1538 (1986).
22. A. Altman, J. M. Cardenas, R. A. Houghten, F. J. Dixon, A. N. Theofilopoulos, *Proc. Natl. Acad. Sci. U.S.A.* **81**, 2176 (1984).
23. G. Ju *et al.*, *J. Biol. Chem.* **262**, 5723 (1987).
24. A. M. Lesk and K. D. Hardman, *Science* **216**, 539 (1982); *Methods Enzymol.* **115**, 381 (1985).

25. Supported by award AI-19762 and Research Career Development Award AI-00631 from NIH to D.B.M. [Ala^{125}]IL-2 is being jointly developed by Amgen, Thousand Oaks, California; Cilag, Schaffhausen, Switzerland; and Ortho Pharmaceutical Corporation, Raritan, New Jersey. Atomic coordinates will be deposited in the Brookhaven Protein Data Bank after completion of refinement.

9 October 1987; accepted 17 November 1987